PHYSICAL REVIEW E VOLUME 54, NUMBER 5 NOVEMBER 1996

Effects of hydrostatic pressure on the monoolein-water system: An estimate of the energy function of the inverted $Ia3d$ cubic phase

Paolo Mariani,[1,3,*] Barbara Paci,[2,3] Peter Bösecke,[4] Claudio Ferrero,[4] Maren Lorenzen,[4] and Roberto Caciuffo[2,3]
[1]*Istituto di Scienze Fisiche, Facoltà di Medicina, Università, Via Ranieri, I-60131 Ancona, Italy*
[2]*Dipartimento di Scienze dei Materiali e della Terra, Università, Via Brecce Bianche, I-60131 Ancona, Italy*
[3]*Istituto Nazionale per la Fisica della Materia, INFM, Research Unit of Ancona, Ancona, Italy*
[4]*European Synchrotron Radiation Facility, POB 220, F-38043 Grenoble Cedex, France*

(Received 13 May 1996)

Synchrotron x-ray diffraction has been used to investigate the mesomorphism of a monoolein-water dispersion under hydrostatic pressure. The results show the existence of a new phase, probably with cubic symmetry, before the transition from the L_α to the L_c lamellar phase occurs. Changes of the lipid bilayer conformation are discussed and the total energy function for the inverted cubic $Ia3d$ and the lamellar L_α mesophase is derived. An estimate of the energy necessary for packing the lipid hydrocarbon chains is given.
[S1063-651X(96)11011-4]

PACS number(s): 87.15.Da, 61.30.Eb, 61.10.Eq, 64.70.Md

The polymorphism of lipids dispersed in water is extraordinarily rich and several phases are frequently observed as the temperature or the concentration are varied. Of particular biological and technological interest are the phases where the hydrocarbon chains assume a highly disordered conformation, and the structure results from the mutual organization of a hydrocarbon continuum separated from water by the head groups of the lipid molecules. They are the systems where cubic phases, the most complex among lipid organizations, are observed [1,2]. Moreover, the conditions for the appearance of cubic phases are so close to those prevailing in living organisms that their biological significance cannot be disregarded. Cubic structures might, for instance, be present in intracellular organelles and are probably involved as local intermediates in several cell processes such as membrane fusion, fat digestion, and metabolism [3–5].

The structural characteristics of these mesophases have been extensively investigated, but the driving forces responsible for their formation are not yet fully understood. The structure of some of the cubic phases may be described in terms of infinite periodic minimal surfaces (IPMS), i.e., infinite arrays of connected saddle surfaces with zero mean curvature at every point [6]. Lipid monolayers are draped across either side of the IPMS, touching it with their terminal methyl groups; the result is a three dimensional periodic bicontinuous structure, formed by distinct water and lipid volumes. The crystallographic space group of the cubic phase determines the type of the corresponding IPMS; the two most common inverse cubic phases (space groups $Ia3d$ and $Pn3m$) are based on the G (gyroid) and D (diamond) surfaces, respectively [6,7]. Recently, the curvature elastic-energy function for the periodic $Ia3d$ cubic phase of hydrated monoolein has been calculated by the osmotic stress method, allowing the stabilities of the different phases to be predicted as a function of composition [8].

In the monoolein-water system, a crystalline lamellar phase L_c and several mesophases have been identified at ambient pressure, including a lamellar structure L_α, where lipid molecules assemble into stacked sheets, an inverted hexagonal phase, which consists of cylindrical structure elements packed on a two-dimensional (2D) hexagonal lattice, and two inverse bicontinuous cubic phases with space group $Pn3m(Q^{224})$ and $Ia3d(Q^{230})$, respectively [1,4,7,9]. Recently, the temperature and pressure dependent phase behavior of monoolein in excess water has also been described [10]. As studies of pressure effects can elucidate the mechanism underlying lipid phase transformations and provide information about the energy contributions that stabilize the different mesophases, we have performed an x-ray synchrotron diffraction experiment on a monoolein sample containing 25 wt % of water and maintained at different pressures, from ambient to about 9 kbar.

The monoacylglyceride 1-monoolein was obtained by Sigma Chemical Co. with purity of >99% and was used without further purification. A mixture containing 25 wt % of bidistilled water was prepared and equilibrated for one day at room temperature and pressure. Diffraction measurements were carried out by using the high-brilliance small angle x-ray scattering camera at the European Synchrotron Radiation Facility (ESRF), Grenoble, France, equipped with a high pressure cell consisting of a cylinder of hardened maraging steel with a perpendicular bore for the x-ray windows [11]. The wavelength of the incident beam was $\lambda = 0.99$ Å and the explored s range ($s = 2\sin\theta/\lambda$, where 2θ is the scattering angle) was between 0.005 and 0.054 Å^{-1}. Diffraction patterns were collected at 20 °C at different pressures, from 1 bar to 9 kbar.

Selected x-ray diffraction patterns, showing a number of reflections, are reported in Fig. 1. By analyzing the spacing ratios of the diffraction peaks, the different phases have been identified, following the usual procedure [1]. Up to a pressure of about 1.0 kbar, three phases coexist in equilibrium.

---

[*] Author to whom correspondence should be addressed: Istituto di Scienze Fisiche, Facoltà di Medicina, Università di Ancona, Via Ranieri 65, I-60131 Ancona, Italy. FAX: 39 71 2204605; Electronic address: Mariani@anvax1.unian.it

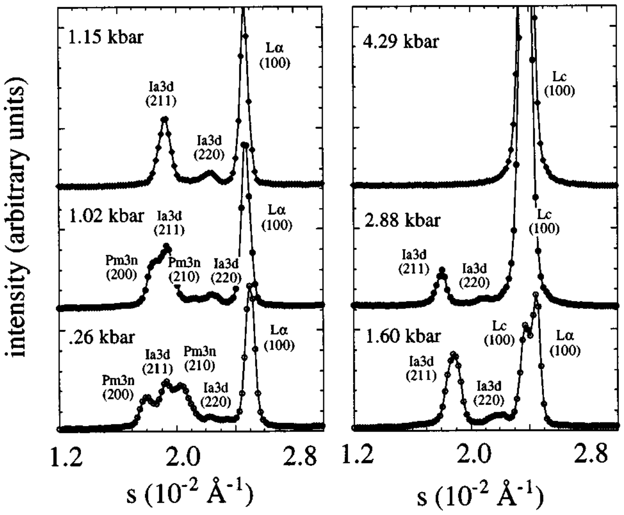

FIG. 1. X-ray diffraction patterns recorded at different pressures.

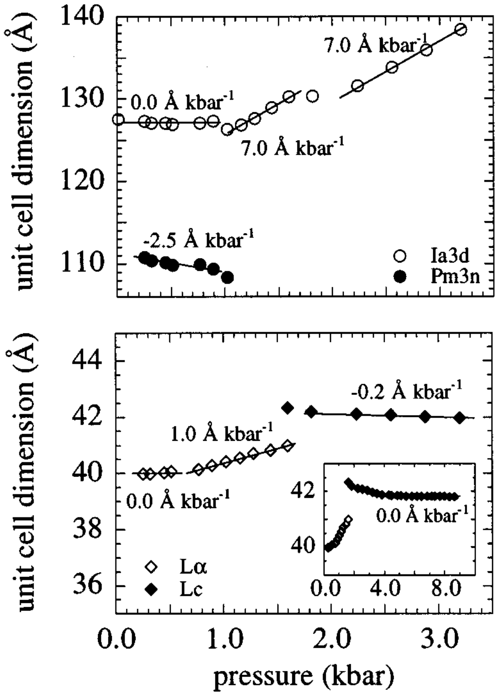

FIG. 2. Pressure dependence of the unit cell dimension of the different mesophases exhibited at room temperature by the monoolein-water (25 wt. %) system. The lattice parameter dependence on pressure (da/dp) is indicated.

The reflections of higher intensities were indexed as (211) and (220) of the cubic lattice of space group $Ia3d$ and as (100) of the L_α lamellar lattice. Two more reflections also occur, which indicate the presence of a mesophase not observed at ambient pressure in the monoolein-water system. Theoretical reasons and the structural characteristics of the lamellar phases suggest that a micellar cubic phase should also be present in the investigated concentration range [9,12]. If cubic symmetry is assumed, the spacing ratios of the extra reflections index to $\sqrt{4}:\sqrt{5}$, and indicate a primitive cubic lattice. Therefore the new phase could have the $Pm3n$ structure (Q^{223}), which has been observed in other lipid systems in the low concentration side of the phase diagram, near the micellar solution [3]. The $Pm3n$ structure consists of two types of micelles, one quasispherical in shape, the other somewhat flattened. All the known examples of the $Pm3n$ phase are of type I (oil in water), but the topology of the nonlamellar phases in the monoolein-water system suggests that in this case the structure consist of water-containing micelles embedded in a hydrocarbon matrix. However, it must be noticed that the number of observed reflections is too small to allow an unambiguous identification of the space group. The extra reflections disappear at about 1 kbar; up to 1.5 kbar, the profiles are consistent with the contemporaneous presence of the $Ia3d$ and L_α phases. At higher pressure, from about 1.5 to 4.5 kbar, the $Ia3d$ phase coexists with the crystalline lamellar L_c phase, which is the only one surviving at even higher pressure, at least up to 8.7 kbar.

The pressure dependence of the lattice parameters is shown in Fig. 2. In the range between ambient pressure and 1.0 kbar, a linear decrease of the repeating unit of the presumed $Pm3n$ phase is observed, at a rate of -2.5 Å /kbar, while the lattice parameter of the L_α and $Ia3d$ phases remains almost constant. At higher pressures, the repeat unit of the lamellar L_α phase increases at a rate of 1 Å /kbar, up to 1.7 kbar, which is the limit of stability of this structure. An expansion of the $Ia3d$ unit cell, with a rate of 7.0 Å /kbar, is also observed. A pressure dependence of 7.3 Å /kbar was found at 20 °C for the lattice parameter of the $Pn3m(Q^{224})$ cubic phase of monoolein in excess water [10], suggesting that the water compressibility plays a small role in the volume variation of the mesophases. After an initial small contraction $(da/dp=-0.2$ Å /kbar), the repeat unit a of the crystalline L_c lamellar phase remains constant, from 4 kbar to the highest reached pressure.

The observed phase sequence and pressure dependence can be understood in terms of simple molecular packing arguments, based on changes in the molecular wedge shape of monoolein. Increasing pressure increases the lipid chain order parameter, and then decreases the molecular wedge shape. This results in an enlargement of the unit cell size of the $Ia3d$ cubic phase because of a decreased curvature of lipid bilayer. The more cylindrical molecular shape also leads to the formation of the lamellar L_α phase, whose unit cell increases as a function of pressure, as the chain order parameter increases. Upon further increasing the pressure, the crystalline L_c phase, which shows the higher lipid packing density, finally forms. This structure is practically incompressible. The occurrence of a metastable micellar phase in passing from the liquid crystalline phases to the crystalline lamellar might reflect some structural anomalies recently observed in the L_α phase under nonequilibrium conditions [9,12]. Nevertheless, a peculiar metastable phase behavior with increasing pressure could be induced by changes in phase composition of the competing structures.

Using the topological constants for the gyroid surface and the equations reported in Ref. [13], the lipid length l in the $Ia3d$ phase has been calculated from the measured lattice parameter, and is reported in Fig. 3, in comparison with the monolayer thickness of the lamellar phases. The increase of l reflects the progressive change of the molecular shape from

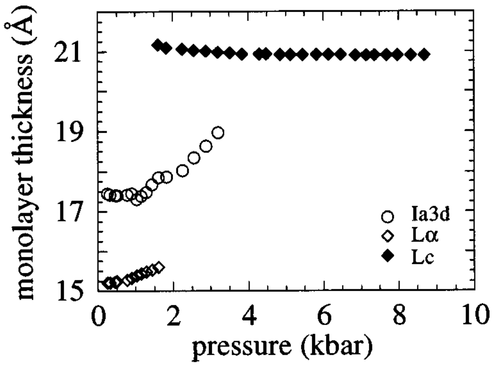

FIG. 3. Pressure dependence of the monolayer thickness for the cubic $Ia3d$ and the lamellar L_α and L_c phases.

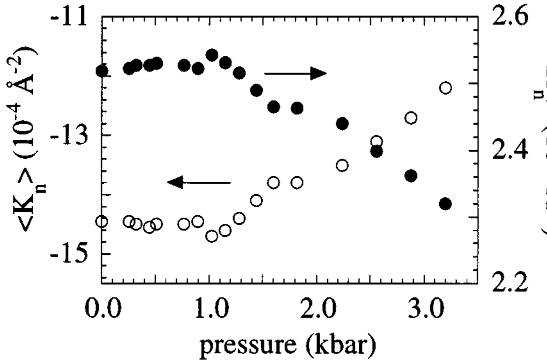

FIG. 5. Pressure dependence of the average over the $Ia3d$ unit cell of the mean curvature $\langle H_n \rangle$ and of the Gaussian curvature $\langle K_n \rangle$, calculated at the head group level.

wedgelike to cylindrical-like, as also indicated by the variation of the cross-sectional area S_{lip} calculated at different distances from the water-lipid interface (Fig. 4). Of particular interest is the absence of the so-called neutral surface, i.e., the surface where the cross-sectional area does not change upon bending [14]. The pressure derivative of S_{lip} (a sort of lateral compressibility) at different levels of the molecular axis is also drawn in Fig. 4, and clearly shows that pressure is more effective in reducing the lateral extension of the lipid near its terminal methyl group than it is at the water interface. From the diffraction data, and the Euler characteristic of the gyroid IPMS [13], the average over the $Ia3d$ unit cell of the mean curvature at the head group level ($\langle H_n \rangle$) and the average of the Gaussian curvature $\langle K_n \rangle$ have been obtained. Figure 5 shows the pressure dependence of these quantities, which could be regarded as a measure of the order parameter for the transitions between different mesophases. The progressive unbending of the lipid bilayer as a function of pressure appears well documented. It must be noticed that all the calculations have been performed under the assumption that the water content is the same in all the phases, and equal to the sample nominal concentration.

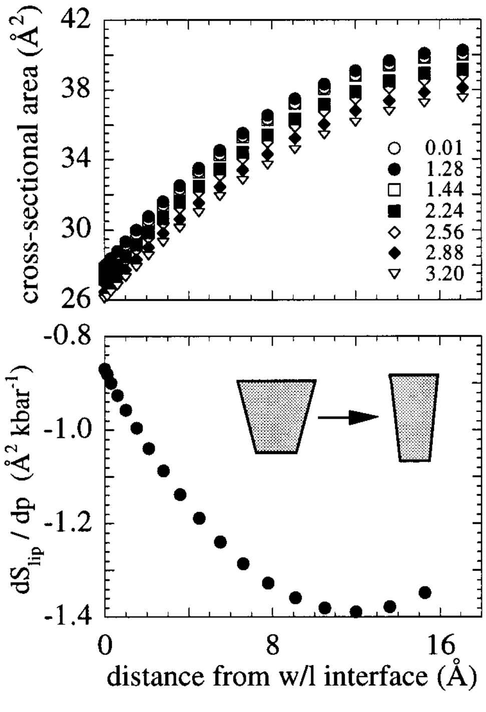

FIG. 4. Top: cross-sectional area S_{lip} calculated at different distances from the water-lipid interface for the cubic $Ia3d$ phase at different pressures (indicated in kbar). Bottom: variation of the cross-sectional area per unit pressure change (dS_{lip}/dp) at different distances from the water-lipid interface. The inset shows schematically the pressure induced molecular shape deformation.

For the $Ia3d$ phase, the total energy function has been derived by numerical integration of the pressure p over the volume V of the cubic unit cell:

$$E(p) = -\int p\,dV + E_0, \tag{1}$$

where p is the external pressure and the volume variation is immediately obtained from the diffraction data. E_0 is the integration constant, fixed at the value determined in Ref. [8]. The so obtained free energy per molecule is reported in Fig. 6 as a function of the pressure.

To give an interpretation of this experimental curve, we will describe the free energy of the lipid layer in terms of various elastic energy contributions, namely, the lateral expansion (or compression) and the curvature terms, as assumed in [4,15–17]:

$$G_{\text{el}}/S_{\text{lip}} = g_S + g_{\text{curv}}, \tag{2}$$

where G_{el} is the elastic energy per molecule. The curvature elastic energy can be written in terms of the mean and Gaussian curvatures of the lipid monolayer [4,8,15,18]:

$$g_{\text{curv}} = 2k_M(\langle H_n^2 \rangle - 2H_0\langle H_n \rangle + H_0^2) + k_G\langle K_n \rangle, \tag{3}$$

where k_M is the rigidity constant, k_G is the Gaussian curvature constant, H_0 is the spontaneous curvature, and $\langle H_n^2 \rangle$ represents the second moment of the mean curvature averaged over the unit cell. $\langle H_n^2 \rangle$, $\langle H_n \rangle$, and $\langle K_n \rangle$ should be evaluated at the same surface [13]. The energy of lateral expansion is [4,16]

$$g_S = \tfrac{1}{2}k_S(S_{\text{lip}}/S_0 - 1)^2, \tag{4}$$

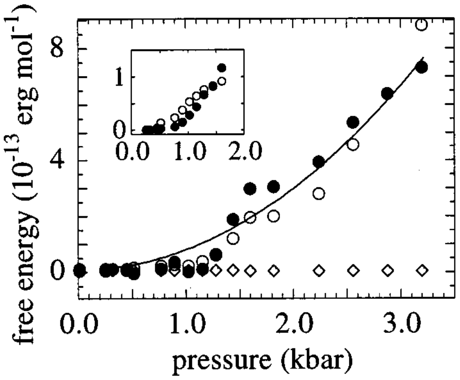

FIG. 6. Experimental total free energy obtained at different pressures for the cubic $Ia3d$ phase (closed circles). Calculated elastic curvature (diamonds) and lateral compression (open circles) energies are also shown. The corresponding data for the lamellar L_α phase are shown in the inset (closed circles, experimental free energy; open symbols, calculated lateral compression energy).

where k_S is the lateral compression modulus, and S_0 is the area per molecule at the polar-nonpolar interface which minimizes the sum of the head group and chain contributions to the free energy. According to Ref. [16], the k_S can be obtained from the second derivative with respect to the area of the free energy function. The present data lead to a k_S value of 532 dyn cm^{-1}. It should be noticed that this value is larger than the one measured for the monoolein monolayer at the air-water interface, $k_S^m = 120$ dyn cm^{-1} [12]: the lateral pressure is effective against the repulsion between the chains and the head groups, which at the concentration used in the present experiment could be reasonably very high.

It is generally assumed that the lateral expansion term is much larger than the curvature term, i.e., deformations involving stretching are more costly energetically than those involving bending. Under this approximation, the equilibrium shape of the membrane could be analyzed taking into account only the curvature energy [4,19]. Recently, the two curvature constants k_M and k_G for the $Ia3d$ cubic phase of hydrated monoolein have been determined at ambient pressure, by fitting Eq. (3) to the free energy obtained as a function of concentration by the osmotic stress method [8].

However, as stressed in Refs. [17,19], the curvature elastic approximation becomes inaccurate when the cubic phase is not sufficiently swollen, and transverse forces make significant contributions to the total free energy. We report in Fig. 6 the calculated lateral compression and the curvature contributions to the free energy per molecule. The curvature term, calculated using Eq. (3) and the constants k_M and k_G obtained in Ref. [8], appears orders of magnitude lower than the observed free energy. By contrast, a fair agreement is observed between the experimental data and the energy of lateral compression calculated using Eq. (4).

For comparison, the free-energy function of the lamellar L_α phase has also been obtained by numerical integration of the pressure p over the thickness of the unit cell. In this case, only the lateral compression term contributes to the free energy. From the second derivation with respect to the area per molecule [16], a k_S value of 444 dyn cm^{-1} is obtained, which is close to the one observed in the $Ia3d$ phase. Then, using Eq. (4), the energy of lateral compression can be calculated and compared with the experimental curve, as shown in the inset of Fig. 6. The good agreement confirms that the pressure affects the equilibrium shape of the membrane mainly through stretching deformation.

[1] P. Mariani, V. Luzzati, and H. Delacroix, J. Mol. Biol. **204**, 165 (1988).
[2] A. Gulik, H. Delacroix, G. Kirschner, and V. Luzzati, J. Phys. (France) II **5**, 445 (1995).
[3] V. Luzzati, R. Vargas, P. Mariani, A. Gulik, and H. Delacroix, J. Mol. Biol. **229**, 540 (1993).
[4] J. M. Seddon, Biochim. Biophys. Acta **1031**, 1 (1990).
[5] J. Nieva, A. Alonso, G. Basanets, F. Goni, A. Gulik, R. Vargas, and V. Luzzati, FEBS Lett. **368**, 143 (1995).
[6] L. E. Scriven, Nature (London) **263**, 123 (1976).
[7] S. T. Hyde, S. Andersson, B. Ericsson, and K. Larsson, Z. Kristallogr. **168**, 213 (1984).
[8] H. Chung and M. Caffrey, Nature (London) **368**, 224 (1994).
[9] J. Briggs, H. Chung, and M. Caffrey, J. Phys. (France) II **6**, 723 (1996).
[10] C. Czeslik, R. Winter, G. Rapp, and K. Bartels, Biophys. J. **68**, 1423 (1995).
[11] M. Lorenzen, C. Riekel, A. Eichler, and D. Häusermann, J. Phys. (France) IV **3**, C8-487 (1993).
[12] P. Mariani and S. Dante (unpublished).
[13] D. C. Turner, Z-G. Wang, S. M. Gruner, D. A. Mannock, and R. N. McElhaney, J. Phys. (France) II **2**, 2039 (1992).
[14] H. Chung and M. Caffrey, Biophys. J. **66**, 377 (1994).
[15] W. Helfrich, Z. Naturforsch. Teil C **28**, 693 (1973).
[16] E. Evans and R. Skalak, *Mechanics and Thermodynamics of Biomembranes* (CRC, Boca Raton, FL, 1980).
[17] R. H. Templer, C. D. Turner, P. Harper, and J. M. Seddon, J. Phys. (France) II **5**, 1053 (1995).
[18] D. M. Anderson, S. M. Gruner, and S. Leibler, Proc. Natl. Acad. Sci. USA **85**, 5364 (1988).
[19] R. H. Templer, J. M. Seddon, and N. A. Warrender, Biophys. Chem. **49**, 1 (1994).